NATURAL FREQUENCIES AND CRITICAL LOADS OF FUNCTIONALLY GRADED SINGLE SPAN BEAMS RESTING ON WINKLER'S ELASTIC FOUNDATION

Nguyen The Truong Phong
GACES, Faculty of Civil Eng. and Applied Mechanics, Univ. of Technical Education HCM City
Nguyen Trong Phuoc
Department of Civil Engineering, Ho Chi Minh City University of Technology

(Received: 08/05/2013; Revised:30/05/2013; Accepted:30/08/2013)

ABSTRACT

Natural frequencies and critical loads of functionally graded single span beams resting on Winkler's elastic foundation with general boundary conditions are presented in this paper. The analytical model of the beam is described by using the first order shear deformation theory, however, the transverse shear stress is derived from expression of the normal stress and equilibrium equation and thus, its shear correction factor is then obtained analytically. The effective material properties of the beam are assumed to follow simple power law form. The governing equation of motion of the beam is derived based on Lagrange's equations with specific boundary conditions satisfied with the Lagrange's multipliers. Comparisons between the results of present study with available results in the literature show a good agreement. In addition, parametric analysis is carried out, including material distribution, boundary conditions and axial load as well as foundation factor and slenderness ratio.

Keywords: Vibration analysis, Buckling analysis, Functionally graded beam, elastic foundation.

Introduction

The development of the materials science now aims to answer to service conditions and it requires that materials performance vary with location within the component. These considerations form the essential elements of the logic underlying the conception of the majority of functionally graded materials (FGMs). They are special composite materials in which material properties vary smoothly and continuously from one surface to the other to achieve the desirable requirements. This is achieved by gradually varying the volume fraction of the constituent materials. Since introduced in the 1980s, FGMs have been used in many technical areas such as aviation, aerospace, defense industry, power and biotechnology. Because of the widespread applications, these structures made of FGMs have attracted the attention. The developments and applications of FGMs after the year 2000 were summarized in the study of Birman *et al* (2007). Different areas are related to various aspects of theory and application of FGM including uniformity of the material, heat transfer problems, stress, stability and dynamic analyses, testing, manufacturing and

design, applications, and fracture are also reflected in this paper.

During the past few decades, frequency and buckling analysis of beam structures has attracted more attention from the scientific community as reflected by increasing number of publications devoted to that. Most of the investigations performed on the buckling problem are concerned with determining the critical buckling loads and their associated mode shapes. Nayfeh and Emam (2008) presented a closed form solution for the post buckling analysis of isotropic beams based on the EBT. They studied critical buckling loads and the associated mode shapes. They also studied the free vibration behavior of the buckled isotropic beams in the postbuckling domain. This type of vibration analysis means investigating the vibration characteristics, which takes place in the vicinity of a buckled configuration. Afterwards, they extended their work and found an exact solution for the post buckling behavior of symmetrically laminated composite beams (Emam and Nayfeh, 2009). They investigated the critical buckling load and free vibration in the postbuckling region. An improved third order shear deformation theory is employed to investigate thermal buckling and vibration of the functionally graded beams is presented in (Wattanasakulpong *et al*, 2011). In this study, the Ritz method is adopted to solve the eigenvalue problems that are associated with thermal buckling and vibration in various types of immovable boundary conditions. Fallah *et al* (2011) presented a simple analytical expression to study nonlinear free vibration and post - buckling analysis of FGM Euler - Bernoulli beams under axial force. Using the same approach and model, they also studied thermo-mechanical buckling and nonlinear free vibration of functionally graded (FG) beams in Fallah *et al* (2012). Rahimi G.H *et al* (2012) investigated the post-buckling behavior of functionally graded Timoshenko beams under general boundary conditions by means of an exact solution method. FG beams are considered to have fixed–fixed, fixed–hinged, and hinged–hinged end conditions. A closed-form solution is achieved for the post-buckling deformation as a function of the exerted axial load that is beyond the critical buckling load. In order to study the vibrations taking place near a buckled equilibrium position, the linear vibration problem is exactly solved around the first buckled configuration of a hinged–hinged FG beam. Mohanty SC *et al* (2010) used the finite element method and Timoshenko beam theory to analyze free vibration and stability of a functionally graded origin beam and a functionally graded sandwich beam on Winkler elastic foundation. However, they mainly focused on the influence of Winkler elastic foundation and material distributions on frequency and critical load of hinged–hinged beams. With the same method, they also investigated the parametric instability of these beams subjected to a dynamic axial load in Mohanty *et al* (2011).

To the best of the author's knowledge, there are some approaches used for static and forced analyses of functionally graded beam, but free vibration and buckling analysis of FG beams on Winkler's elastic foundation with general boundary conditions based on Lagrange's equations have been not presented in literature. In present paper, Lagrange's equations with specific boundary conditions satisfied with Lagrange's multipliers are used to formulate the governing equation of motion of the pinned – pinned, pinned – clamped and clamped - clamped beams. The analytical model of the beam is described by using Timoshenko beam theory and Von-Karman relationships for

material behavior, but shear correction factor is determined analytically. The material properties of the beams are assumed to follow simple power law form. Some numerical examples are carried out to study the influences of some parameters of beams on vibration and instability behaviors.

Formulation

Beam model

In this paper, FG beams affected by an axial load N_x on Winkler's elastic foundation have been investigated. The length of the beams is L; thickness is h and width is b, with co-ordinate system Oxz having the Origin O shown in Fig. (1). The Winkler foundation has elastic factor per unit length of the beam k_z.

Figure 1. A hinged – hinged FG beam on Winkler's elastic foundation

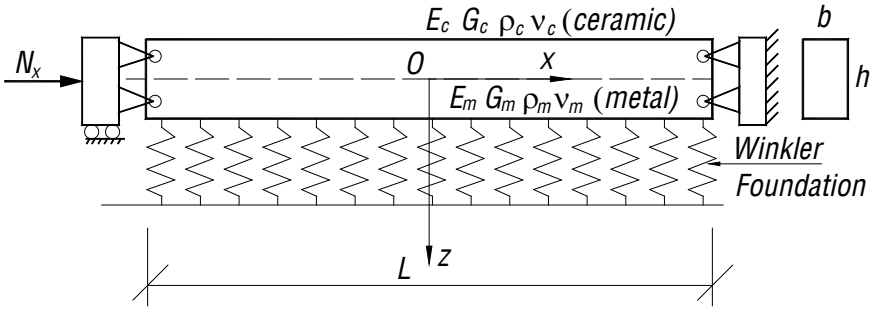

The effective material properties of FG beam, including Young's modulus E, Poisson's ratio ν and shear modulus G as well as mass density ρ, grade continuously in the thickness direction according to power-law distribution in terms of the volume fractions of the compositions (Wakashima *et al*, 1990) as follows:

$$P = (P_b - P_t)\left(\frac{z}{h} + \frac{1}{2}\right)^k + P_t \quad (1)$$

where, P is the effective material properties of FG beam; P_t and P_b are the effective material properties of the top – layer (ceramic) and bottom – layer (metal) constituents, respectively; k is the volume fraction exponent that is the positive real value.

It is clear from Eq. (1) that when $z = -h/2, P = P_c$, and when $z = h/2, P = P_m$.

Base on Timoshenko beam theory, the displacement fields are shown as:

$$u(x,t) = u_0(x,t) + z\phi_0(x,t)$$
$$w(x,t) = w_0(x,t) \quad (2)$$

where $u(x,t), w(x,t)$ are axial and transverse displacements of any point of beam, respectively; $u_0(x,t), w_0(x,t)$ are axial and transverse displacement in the middle line, respectively; and ϕ_0 is the rotation of cross-section, t denotes time.

According to Von-Karman's relationships, the normal strain ε_{xx}, the shear strain γ_{xz}, and the curvature κ_x of the beam are presented as:

$$\varepsilon_{xx} = \frac{\partial u_0}{\partial x} + \frac{1}{2}\left(\frac{\partial w_0}{\partial x}\right)^2 + z\frac{\partial \phi_0}{\partial x} \qquad \gamma_{xz} = \frac{\partial w_0}{\partial x} + \phi_0 \qquad \kappa_x = \frac{\partial \phi_0}{\partial x} \quad (3)$$

From Eq. (3), we can see that the relationship between strain and displacement is nonlinear due to the effect of large displacement. In the case of the displacement is very small, $(\partial w_0/\partial x)^2 \approx 0$ so the behavior is linear.

The normal and shear stresses are given by:

$$\sigma_{xx} = E(z)\varepsilon_{xx} \quad \tau_{xz} = k_s G(z)\gamma_{xz} \tag{4}$$

and internal axial force N_x, shear force Q_z, bending moment M_y are presented by:

$$N_x = A_{xx}\left[\frac{\partial u_0}{\partial x} + \frac{1}{2}\left(\frac{\partial w_0}{\partial x}\right)^2\right] + B_{xx}\frac{\partial \phi_0}{\partial x} \qquad M_y = B_{xx}\left[\frac{\partial u_0}{\partial x} + \frac{1}{2}\left(\frac{\partial w_0}{\partial x}\right)^2\right] + D_{xx}\frac{\partial \phi_0}{\partial x} \qquad Q_z = k_s A_{xz}\left[\frac{\partial w_0}{\partial x} + \phi_0\right] \tag{5}$$

where, $A_{xx}, B_{xx}, D_{xx}, A_{xz}$ are extensional, coupling, bending and shear rigidities, respectively and taken as the following forms:

$$\left(A_{xx} \quad B_{xx} \quad D_{xx}\right) = \int_A E(z)\left(1 \quad z \quad z^2\right)dA \qquad A_{xz} = \int_A G(z)dA \tag{6}$$

and k_s is the shear correction factor and is usually taken the 5/6 value as homogeneous rectangular cross – section. Nevertheless, in this paper, it is exactly calculated from equilibrium equation, $\frac{\partial \sigma_{xx}}{\partial x} + \frac{\partial \sigma_{xz}}{\partial z} = 0$, leading to:

$$k_s = \frac{1}{A_{xz}}\left(\int_A \frac{\left(bA_z(z) + dB_z(z)\right)^2}{G(z)}dA\right)^{-1} \tag{7}$$

with

$$\left[A_z(z) \quad B_z(z)\right] = \int_A E(\xi)(1 \quad \xi)dA \qquad b = \frac{B_{xx}^2}{B_{xx}^2 - A_{xx}D_{xx}} \qquad d = \frac{-A_{xx}^2}{B_{xx}^2 - A_{xx}D_{xx}} \tag{8}$$

It is from Eq. (7) that the shear correction factor k_s is not constant and depends on the effective material properties and material contrast (E_c / E_m) of the FG beams. This phenomenon is detailed in Table I showing the variation of shear correction factor with difference values of power – law exponent k and the ratio between ceramic's Young modulus E_c and metal's Young modulus E_m. As expected, the traditional shear correction factor ($k_s = 5/6 = 0.8333$) is recovered in two cases $n = 1$ and $k = 0$, which corresponds to homogeneous beams.

Table 1. Variation of shear correction factor with power – law exponent k and E_c / E_m ratio

k	$n = E_c / E_m$					
	1	5	38/7	8	10	15
0	0.8333	0.8333	0.8333	0.8333	0.8333	0.8333
1	0.8333	0.8304	0.8304	0.8308	0.8312	0.8319
2	0.8333	0.8596	0.8602	0.8625	0.8634	0.8645
5	0.8333	0.8674	0.8678	0.8693	0.8698	0.8703
8	0.8333	0.8582	0.8584	0.8593	0.8595	0.8598
10	0.8333	0.8532	0.8534	0.8541	0.8542	0.8544

Equation of motion systems

The Lagrangian functional of problem (Clough *et al*, 1993) is given by:

$$\prod = K - U + W + \sum \lambda_m f_m(x\,t) \qquad (9)$$

where are the Lagrange multipliers which are also support reactions; $f_m(x,t)$ are the equations of constrain for general boundary condition cases showing in Table II; K is kinetic energy; U is strain energy and W is work done of beam on elastic foundation with the effect of axial load. They are presented by:

$$K = \frac{1}{2}\int_L \left\{ I_A \left[\left(\frac{\partial u_0}{\partial t}\right)^2 + \left(\frac{\partial w_0}{\partial t}\right)^2 \right] + 2I_B \frac{\partial u_0}{\partial t}\frac{\partial \phi_0}{\partial t} + I_D \left(\frac{\partial \phi_0}{\partial t}\right)^2 \right\} dx$$

$$W = \frac{1}{2}\int_L k_z w_0(x,t) w_0(x,t)\,dx - \frac{N_x}{2}\int_L \left(\frac{\partial w_0}{\partial x}\right)^2 dx \qquad (10)$$

$$U = \frac{1}{2}\int_L \left\{ A_{xx}\left[\frac{\partial u_0}{\partial x} + \frac{1}{2}\left(\frac{\partial w_0}{\partial x}\right)^2\right]^2 + 2B_{xx}\frac{\partial \phi_0}{\partial x}\left[\frac{\partial u_0}{\partial x} + \frac{1}{2}\left(\frac{\partial w_0}{\partial x}\right)^2\right] + k_s A_{xz}\left(\frac{\partial w_0}{\partial x} + \phi_0\right)^2 + D_{xx}\left(\frac{\partial \phi_0}{\partial x}\right)^2 \right\} dx$$

In which k_z is Winkler's elastic foundation factor.

In this paper, the displacement functions can be approximated by using space - dependent polynomial terms $x^0, x^1, x^2, ..., x^{N-1}$ and time - dependent generalized coordinates a_n, b_n, c_n in order to apply Lagrange equations (Clough *et al*, 1993) and let as

$$w_0(x,t) = \sum_1^N a_n(t) x^{N-1} \quad ; \quad u_0(x,t) = \sum_1^N b_n(t) x^{N-1} \quad ; \quad \phi_0(x,t) = \sum_1^N c_n(t) x^{N-1} \qquad (11)$$

The governing equations will be derived by using Lagrange equations (Clough *et al*, 1993) are given as follows

$$\frac{\partial \prod}{\partial q_n} - \frac{d}{dt}\frac{\partial \prod}{\partial \dot{q}_n} = 0 \quad ; \qquad n = 1,2,...,3N+4 \qquad (12)$$

where q_n are defined as:

$$\begin{aligned} q_n &= a_n, && n = 1,2,...,N \\ q_n &= b_{n-N}, && n = N,...,2N \\ q_n &= c_{n-2N}, && n = 2N,...,3N \\ q_{3N+m} &= \lambda_m \end{aligned} \qquad (13)$$

After substituting Eq. (11) into Eq. (10) and then using the Lagrange's equations given by Eq. (12), the coupled systems of equations of motion of a hinged – hinged beam as follows

$$\begin{bmatrix} \left[K_{11}^{L}\right]_{NxN}+\left[K^{W}\right]_{NxN}-\left[K^{G}\right]_{NxN} & [0]_{NxN} & \left[K_{13}^{L}\right]_{NxN} & \left[K_{14}^{R}\right]_{Nx4} \\ [0]_{NxN} & \left[K_{22}^{L}\right]_{NxN} & \left[K_{23}^{L}\right]_{NxN} & \left[K_{24}^{R}\right]_{Nx4} \\ \left[K_{31}^{L}\right]_{NxN} & \left[K_{32}^{L}\right]_{NxN} & \left[K_{33}^{L}\right]_{NxN} & [0]_{Nx4} \\ \left[K_{41}^{R}\right]_{4xN} & \left[K_{42}^{R}\right]_{4xN} & [0]_{4xN} & [0]_{4x4} \end{bmatrix} \begin{Bmatrix} a_n(t) \\ b_n(t) \\ c_n(t) \\ \lambda_m(t) \end{Bmatrix} + \\ + \begin{bmatrix} \left[K_{11}^{NL}(a_n(t))\right]_{NxN} & \left[K_{21}^{NL}(a_n(t))\right]_{NxN} & \left[K_{31}^{NL}(a_n(t))\right]_{NxN} & [0]_{Nx4} \\ \left[K_{21}^{NL}(a_n(t))\right]_{NxN} & [0]_{NxN} & [0]_{NxN} & [0]_{Nx4} \\ \left[K_{31}^{NL}(a_n(t))\right]_{NxN} & [0]_{NxN} & [0]_{NxN} & [0]_{Nx4} \\ [0]_{4xN} & [0]_{4xN} & [0]_{4xN} & [0]_{4x4} \end{bmatrix} \begin{Bmatrix} a_n(t) \\ b_n(t) \\ c_n(t) \\ \lambda_m(t) \end{Bmatrix} + \\ + \begin{bmatrix} [M_{11}]_{NxN} & [0]_{NxN} & [0]_{NxN} & [0]_{Nx4} \\ [0]_{NxN} & [M_{22}]_{NxN} & [M_{23}]_{NxN} & [0]_{Nx4} \\ [0]_{NxN} & [M_{32}]_{NxN} & [M_{33}]_{NxN} & [0]_{Nx4} \\ [0]_{4xN} & [0]_{4xN} & [0]_{4xN} & [0]_{4x4} \end{bmatrix} \begin{Bmatrix} \ddot{a}_n(t) \\ \ddot{b}_n(t) \\ \ddot{c}_n(t) \\ 0 \end{Bmatrix} = \begin{Bmatrix} 0 \\ 0 \\ 0 \\ 0 \end{Bmatrix} \tag{14}$$

where $\left[K_{ij}^{L}\right]$ are linear stiffness matrices, $\left[K_{ij}^{NL}\right]$ are nonlinear stiffness matrices which are dependent on generalized coordinate $a_n(t)$, $\left[M_{ij}\right]$ are mass matrices and two rest of matrices $\left[K_{ij}^{R}\right]$ and $\left[K^{W}\right]$ exist due to Lagrange multipliers and Winkler's elastic foundation, respectively; $\left[K^{G}\right]$ are geometric stiffness matrices owing to the effect of axial load.

The terms of matrices $\left[K_{ij}^{G}\right]$, $\left[K_{ij}^{W}\right]$ are given by:

$$K_{ij}^{G} = N_x \int_{-L/2}^{L/2} \left(x^{i-1}\right)' \left(x^{j-1}\right)' dx, \quad i,j = 1,2,...,N$$
$$K_{ij}^{W} = k_z \int_{-L/2}^{L/2} x^{i-1} x^{j-1} dx, \quad i,j = 1,2,...,N \tag{15}$$

and the terms of other matrices in Eq. (14) can be referred to Simsek (2010) and Nguyen and Nguyen (2012).

Table 2. Equations of constrain with different boundary conditions

Boundary conditions	Equations of constrain
Hinged – Hinged (H-H)	$w_0(-L/2,t)=0;\ w_0(L/2,t)=0;\ u_0(-L/2,t)=0;$ $u_0(L/2,t)=0$
Hinged – Clamped (H-C)	$w_0(-L/2,t)=0;\ w_0(L/2,t)=0;\ u_0(-L/2,t)=0;$ $u_0(L/2,t)=0;\ \phi_0(L/2,t)=0$
Clamped – Clamped (C-C)	$w_0(-L/2,t)=0;\ w_0(L/2,t)=0;\ u_0(-L/2,t)=0;$ $u_0(L/2,t)=0;\ \phi_0(L/2,t)=0;\ \phi_0(-L/2,t)=0$

Solution algorithm

The shortened form of the governing equation Eq. (13) is written as follows

$$[M]\left\{\ddot{q}(t)\right\}+\left[K^{L}+K^{W}-K^{G}+K^{NL}\left(q(t)\right)\right]\left\{q(t)\right\}=0 \tag{16}$$

where $q(t)=\left\{a(t)\quad b(t)\quad c(t)\quad \alpha(t)\right\}^{T}$

For free vibration analysis, the time – dependent generalized coordinates can be express as $q(t)=\bar{q}e^{i\omega t}$ and the matrices $K^{NL}(q(t))$ is set to zero in Eq.(16), this situation results in a set of frequency equation that can be shown on following form with ω is the natural frequency of the beam:

$$\left(K^{L}+K^{W}-K^{G}\right)\bar{q}-\omega^{2}\bar{q}M=0 \tag{17}$$

It is noted that the axial force and Winkler's elastic foundation factor appear in the dynamic equation allows to investigate their effect on free vibration behaviors. Eq. (17) is general form for vibration of axially loaded FG beams, which can be used to calculate the natural frequencies, load-frequency interaction curves. In fact, it is found from the condition that the determinant of the system of equations given by Eq. (16) must vanish.

$$\left|\left(K^{L}+K^{W}-K^{G}-\omega^{2}M\right)\right|=0 \tag{18}$$

For stability analysis, the value of buckling load N_{cr} is determined by solving the following equation:

$$\left|\left(K^{L}+K^{W}-K^{G}\right)\right|=0 \tag{19}$$

A step – by – step of solution algorithm is presented in a flowchart form in Fig (2). Based on this algorithm, a computer program using Matlab was developed to calculate both natural frequency and critical load. The accuracy of the program will be verified next.

Figure 2. Flowchart of solution algorithm

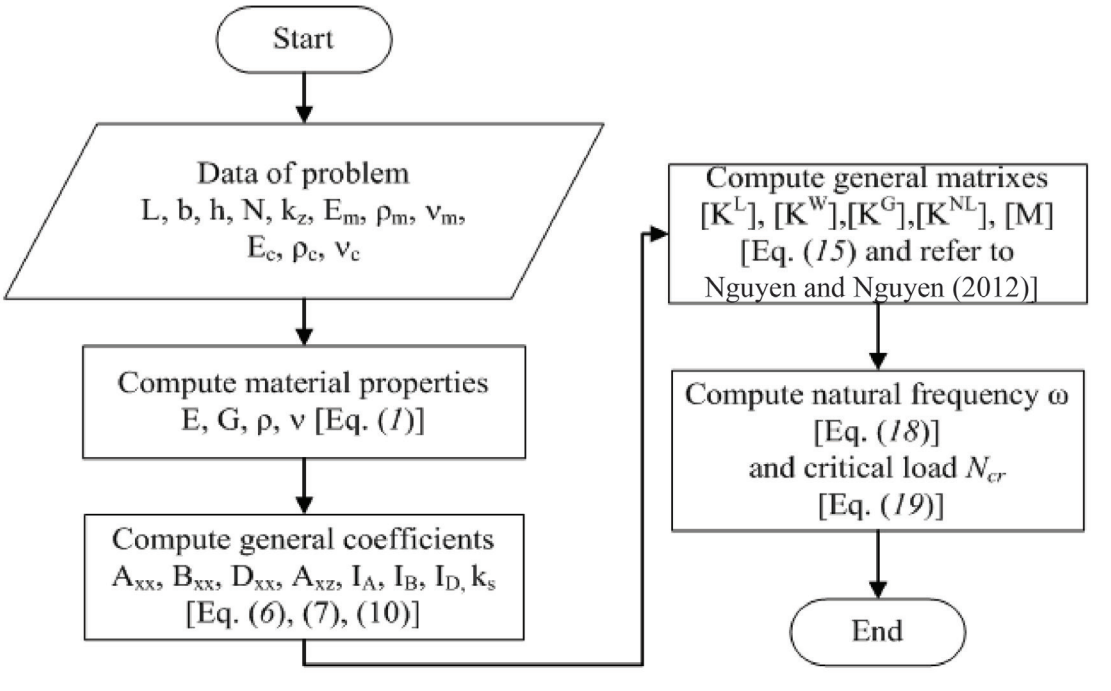

Numerical examples

In this paper, two numerical examples are presented and discussed to verify the convergence and accuracy of the proposed program. Especially, the free vibration and buckling analysis of FG Timoshenko beam acted on elastic foundation are thoroughly investigated through some examples. Some non – dimensional parameters have been used in this paper as follows the non – dimensional Winkler's modulus $\alpha = k_z L^4 / E_m I$, the dimensionless fundamental frequency $\lambda_i = \omega_i L^2 \sqrt{\rho\ A / E_m I}$ and non – dimensional buckling load $\gamma = N_{cr} L^2 / \left(\pi^2 E_m I\right)$.

It is again noted that all effective material properties of FG beams, including Young's modulus E, Poisson's ratio ν and shear modulus G as well as mass density ρ, are the functions of volume fraction exponent k and change continuously along with beam thickness, showing as Eq.(1). If assuming that beams make of metal

$(E_m = 70GPa, \rho_m = 2700kg/m^3, \nu_m = 0.3)$

and ceramic

$(E_c = 380GPa, \rho_c = 5700kg/m^3, \nu_c = 0.3)$,

the variation of the non – dimensional effective material properties along the thickness of beam are displayed in Fig. (3). It can be seen that effective material properties vary quickly near the lowest surface for $k < 1$ and increase quickly near the top surface for $k > 1$. Moreover, effective material properties change linearly along the thickness of beam when $k = 1$ and nonlinearly when $k \neq 1$.

Figure 3. Variation of the dimensionless Young's modulus E and mass density ρ along the thickness of beam

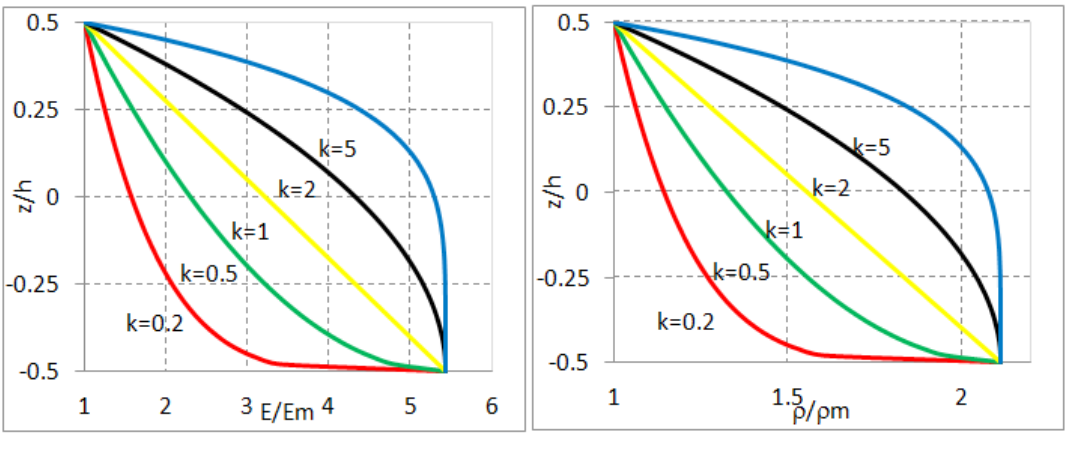

Verifying the convergence

Table 3 shows the non - dimensional frequencies of FG beam for various numbers of terms in displacement functions N in different boundary conditions and L/h ratios when $b = 0.5\text{m}, \alpha = 100, k = 2$, whereas Table 4 present the non - dimensional buckling load at the same conditions in order to study the convergence. Both examples are investigated in two cases, shear correction factor k_s is 5/6 as homogenous section and is calculated analytically as Eq.(7). From these tables, we can see that in terms of $N = 8$ the numerical results are convergent, so $N = 8$ is used for the following examples. Clearly, there are the differences in researched parameters between traditional model $(k_s = 5/6)$ and proposed one. This difference, thus, can be taken into account for accurate analysis of FG beam, especially when slenderness ratio of beam is quite small. It is also noted that the hinged – hinged (H-H) beam has the lowest frequency and critical load while a

beam with clamped – clamped (C-C) end condition has the highest ones. Moreover, for all different kind of beam, there are a slight growth in both non - dimensional frequencies and buckling loads owing to the increase in L/h ratio.

Table 3. Non - dimensional frequencies of FG beam for various boundary conditions and L/h ratio

N	k_s	Hinged-Hinged			Hinged-Clamped			Clamped - Clamped		
		L/h=5	L/h=10	L/h=20	L/h=5	L/h=10	L/h=20	L/h=5	L/h=10	L/h=20
4	5/6	15.949	16.987	17.416	22.366	26.408	28.472	33.201	56.261	105.15
	Eq.(7)	15.976	17.000	17.421	22.466	26.474	28.498	33.561	57.015	106.75
8	5/6	15.305	15.839	15.988	20.279	21.884	22.368	26.429	29.897	31.048
	Eq.(7)	15.319	15.844	15.989	20.329	21.901	22.373	26.539	29.939	31.051
10	5/6	15.304	15.839	15.988	20.279	21.884	22.368	26.429	29.897	31.048
	Eq.(7)	15.319	15.844	15.989	20.329	21.901	22.373	26.539	29.939	31.051

Table 4. Non - dimensional buckling load of FG beam for various boundary conditions and L/h ratio

N	k_s	Hinged-Hinged			Hinged-Clamped			Clamped - Clamped		
		L/h=5	L/h=10	L/h=20	L/h=5	L/h=10	L/h=20	L/h=5	L/h=10	L/h=20
4	5/6	4.6042	5.1275	5.3602	7.6949	9.625	10.516	19.677	56.087	195.29
	Eq.(7)	4.6199	5.1358	5.3631	7.7502	9.657	10.527	20.110	57.603	201.26
8	5/6	4.2943	4.5173	4.5784	6.520	7.291	7.519	10.470	12.740	13.483
	Eq.(7)	4.3030	4.5198	4.5791	6.548	7.301	7.521	10.626	12.785	13.513
10	5/6	4.2943	4.5173	4.5784	6.520	7.291	7.519	10.470	12.740	13.483
	Eq.(7)	4.3030	4.5198	4.5791	6.548	7.301	7.521	10.626	12.785	13.513

Validating the accuracy of present program

The two following examples aim at verifying the accuracy of present formulation and computer program. The first example calculates the first three non - dimensional frequencies for different dimensionless axial loads and Winkler's elastic factors and then compare with the results presented in studies of Cheng *et al* (1988) and Yokoyamat (1996). The second example determines and validates the fundamental buckling loads of FG beam under various boundary conditions with those of Rahimi (2012). These comparisons are provided in both Table 5 and Table 6. As seen from these tables, the present study is very close to the results given in those papers, and the differences can be negligible.

Buckling and free vibration analysis

Fig.5 shows the variation of non - dimensional buckling loads γ of three different beams (C-C, H-C, H-H) with a range values of k in relation to various L/h ratios ($L/h = 5,10,20$) for $\alpha = 100, E_c/E_m = 10$. From this figure, it is concluded that for all boundary conditions, there is a significant increase in the value γ when k rise from 0 to 2, and then this trend continues happening with relative amplitude. As mentioned before, C-C beams have the greatest buckling

loads and H-H beams have the smallest ones. Plus, the effect of power-law index and L/h ratios on H-H beams is by far smaller than C-C beams. Additionally, non - dimensional critical loads rise as L/h ratios increase for all given cases, whereas C-C beam has the biggest rate.

Table 5. The first three non - dimensional frequencies with buckling load γ and Winkler's modulus α for $L/\sqrt{I/A}=10$

Modes No	α	γ	Hinged - Hinged			Hinged - Clamped		
			Exact solution (Cheng 1988)	Yokoyamat (1996)	Present study	Exact solution (Cheng 1988)	Yokoyamat (1996)	Present study
1st	0	0	8.21	8.22	8.215	10.63	10.63	10.627
		0.6	3.47	3.47	3.467	7.32	7.33	7.324
	$0.6\pi^4$	0.6	8.21	8.22	8.216	10.46	10.49	10.482
2nd	0	0	24.23	24.31	24.229	25.62	25.71	25.617
		0.6	19.22	19.31	19.222	20.93	21.03	20.932
	$0.6\pi^4$	0.6	20.59	20.67	20.591	22.20	22.30	22.208
3rd	0	0.6	35.08	35.48	35.176	35.7	36.16	35.853
	$0.6\pi^4$	0.6	35.86	36.25	35.952	36.50	36.90	36.609

Table 6. Fundamental buckling load for FG beam under various boundary conditions (L=0.4m, h=0.04m, b=0.08m)

Fundamental buckling load 10^4kN	k=0	k=2	k=4	k=8	k=10
Clamped - Clamped	Relative error max =0.8%				
G.H. Rahimi (2012)	3.96	2.80	2.66	2.53	2.49
Present study	3.918	2.751	2.624	2.513	2.471
Clamped - Hinged	Relative error max =1.5%				
G.H. Rahimi (2012)	2.12	1.50	1.43	1.37	1.34
Present study	2.088	1.476	1.409	1.349	1.326
Hinged - Hinged	Relative error max =0.7%				
G.H. Rahimi (2012)	1.07	0.75	0.72	0.69	0.68
Present study	1.07	0.765	0.727	0.685	0.675

The relative errors of non - dimensional buckling loads between traditional model $k_s = 5/6$ and proposed model are displayed in Fig.6. Although the fact that relative error is quite small, the increase in the power - law exponent in turn leads to the dramatic increase in this value, standing at the highest point when $k = 4$ after that it levels off for all beams. Interestingly, C-C beams have the biggest error, while H-H beams show the smallest ones.

Figure 4. Variation of dimensionless buckling loads with k for α=100, different boundary conditions

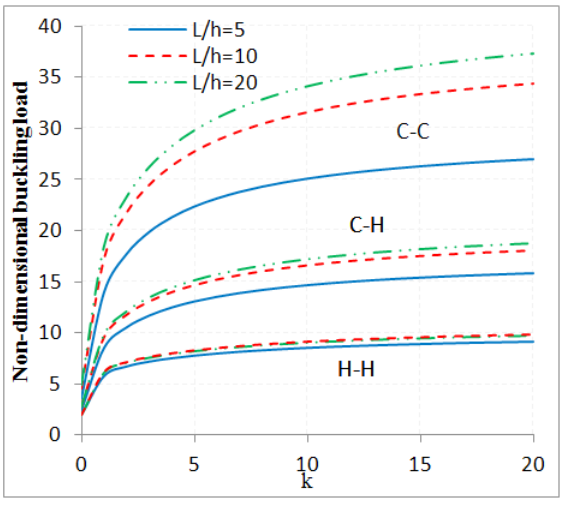

Figure 5. Relative error (0.1%) of dimensionless buckling load with k for for a=100, L/h=5 and different boundary conditions

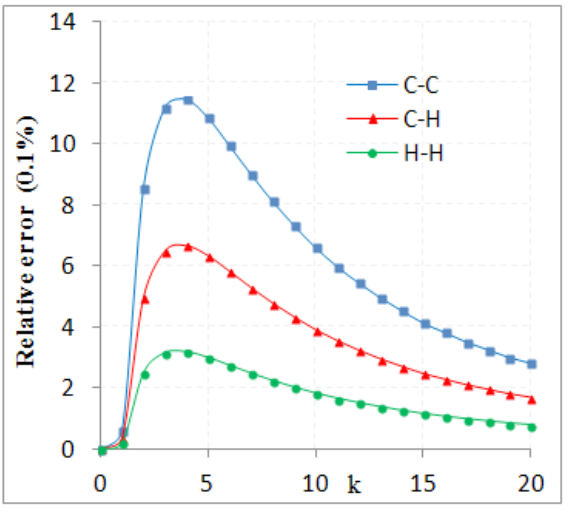

The differences of non - dimensional buckling loads of H-C beams with the different values of k in case of four L/h ratios $(L/h=10,20,30,40)$ and $\alpha=10,100$ are presented in Fig.6 The most striking feature of this figure is that since the increase in the power - law exponent in turn leads to the dramatic increase in non - dimensionals buckling loads, especially when $k\le 1$. It can be also observed that there is a rise in non – dimensional buckling load γ as the values of α go up and the growth rate is equal for all given L/h ratios. By this I mean, the effect of Winkler foundation on critical load is linear. This upward trend also happens as the length to thickness ratio rises to 20 and then it level off for all the values of α.

Fig.7 gives the information about dimensionless buckling loads γ with L/h ratios for $\alpha=100$, $k=1,2,5$ under general boundary conditions (C-C, H-C, H-H). As mentioned before, there is a rise in the value of γ with the increase in the value of k for all given boundary condition. Interestingly, C-C beams have the biggest growth rates, while H-H beams show the smallest ones. It also demonstrates that when $L/h\ge 20$ the figure of γ remains stable for every such a beam.

Figure 6. Variation of dimensionless buckling loads of H-C beam with k for various L/h ratios and α.

- - - -α =100, — α =10

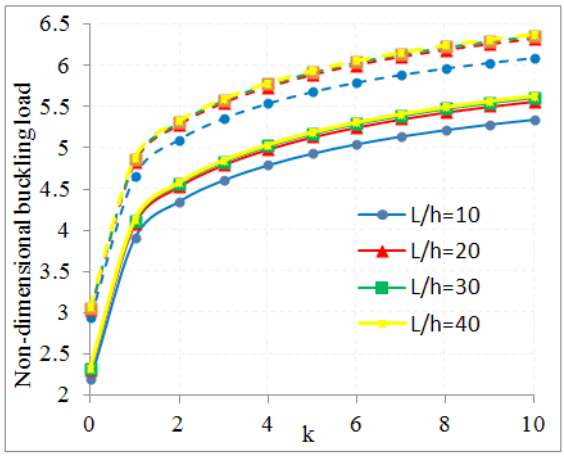

Figure 7. Variation of dimensionless buckling loads with L/h ratios for α=100, various k and different boundary conditions

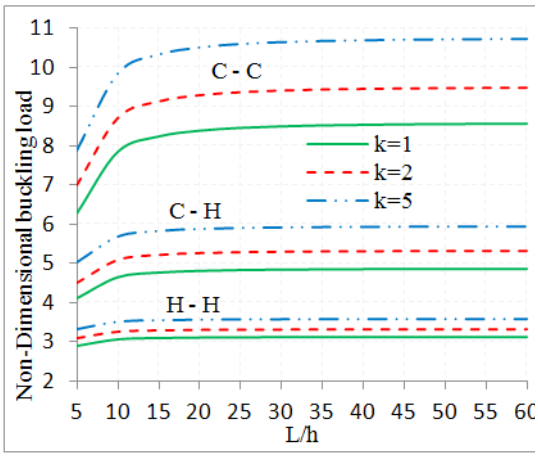

Figure 8. Variation of dimensionless fundamental frequencies of H-H beam with dimensionless axial loads for a=10, L/h=20 and various k

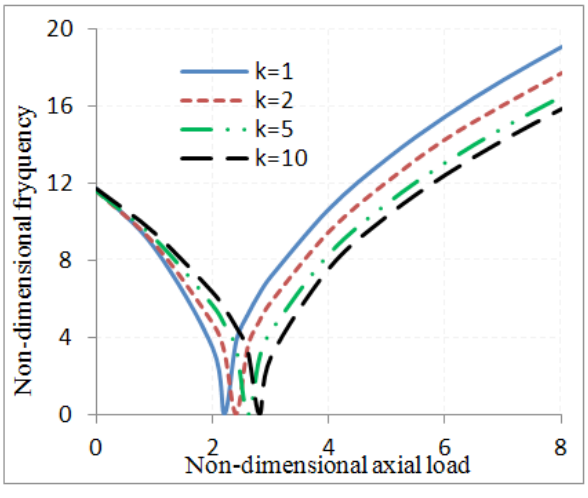

Figure 9. Variation of dimensionless fundamental frequencies with dimensionless axial loads for a=100, L/h=20, k=1 and various boundary conditions

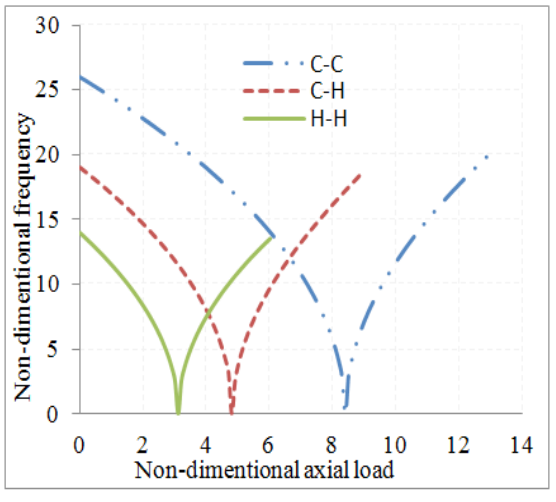

Fig.8 represents the dimensionless fundamental frequencies H-H beam with dimensionless axial loads γ in terms of $\alpha = 10, L/h = 20$ and $k = 1,2,5,10$, whereas these ralationships under different boundary conditions in the case $\alpha = 100, L/h = 20, k = 1$ are highlighted in Fig.10. The frequencies result in different values of k (Fig.9) and each type of boundary condition (Fig.9) declines to zero at its critical load before going up after that load. Clearly, there is a rise in the value of γ and λ with the increase in the value of k for all given boundary condition. Again, C-C beam has the largest dimensionless fundamental frequencies and dimensionless buckling loads.

Conclusion

Free vibration and stability analysis of functionally graded beams on Winkler's elastic foundation with general boundary conditions have been investigated. Comparisons between the results obtained by in this study with available results in the literature show a good agreement. The analysis has also been performed to investigate the effects of boundary conditions, axial load, material distribution and shear correction factor as well as Winkler foundation factor together with slenderness ratio on buckling load and natural frequency of FG beams. It is found that shear correction factor of FG beam is not exactly 5/6 as homogenous beam and it can effect on responses of beam especially C-C beam with small slender ratios. In addition, rising length to thickness ratios up to 20 leads the significant increase in both dimensionless fundamental frequency and buckling load; however, these values remain almost stable once this ratio is over 20. Similarly, there is also a growth in non-dimensional fundamental frequency and critical load as Winkler foundation factor and material distribution factor go up. Whereas the dramatic influence of the latter happened in the case $k \le 1$ for all beams, the former's effect is linear. Moreover, the by far highest values of natural frequency and buckling load belong to C-C beam, followed by C-H beam and H-H beam in the order. Not only that, C-C beam is also the most sensitive one that means that the changes of its frequency and buckling load are strongest whether other research parameters increase or decrease compared to two rest beams. As expected, the first natural frequency drops to zero at critical load.

REFERENCES

[1] Birman V, Byrd LW (2007). Modeling and analysis of functionally graded materials and structures. *Appl Mech Rev*, 60, pp.195–216.

[2] Cheng F. Y. and C. P. Pantelides (1988). Dynamic Timoshenko beam-columns on elastic media. *ASCE J. Structural Engineering*, 114, pp. 1524-1550.

[3] Clough R.W, Penzien J. (1993), *Dynamics of Structures* (Second edition). McGraw – Hill.

[4] Emam SA, Nayfeh AH (2009). Postbuckling and free vibration of composite beams. *Composite Structures*, 88, pp.636–42.

[5] Fallah A, Aghdam MM (2011). Nonlinear free vibration and post-buckling analysis of functionally graded beams on nonlinear elastic foundation. *European Journal of Mechanics A/Solids*, 30, pp. 1-13.

[6] Fallah A, Aghdam MM (2012). Thermo-mechanical buckling and nonlinear free vibration analysis of functionally graded beams on nonlinear elastic *Compos B: Eng,* 43, pp. 1523–30.

[7] Mohanty SC, Dash R.R, Rout T (2010). Static and dynamic analysis of a functionally graded Timoshenko beam on Winkler's elastic foundation. *Journal of Engineering Research and Studies*, 1, pp. 149 – 165.

[8] Mohanty SC, Dash R.R, Rout T (2011). Parametric instability of a functionally graded Timoshenko beam on Winkler's elastic foundation. *Nuclear Engineering and Design*, 241, pp. 2698-2715.

[9] Nguyen The Truong Phong, Nguyen Trong Phuoc (2012). Geometrically nonlinear responses of a functionally graded beam on winkler foundation under a moving harmonic load, *Proceeding of the International Conference on Advances in Computational Mechanics* (ACOME), Ho Chi Minh City, Vietnam.

[10] Nayfeh AH, Emam SA (2008). Exact solutions and stability of the postbuckling configurations of beams *Nonlinear Dynamic*, 54, pp.395–408.

[11] Nuttawit Wattanasakulpong, Gangadhara Prusty B, Kelly D W (2011). Thermal buckling and elastic vibration of third-order shear deformable functionally graded beams. *International Journal of Mechanical Sciences*, 53**,** pp. 734–743.

[12] Rahimi G.H, Gazor M.S, M. Hemmatnezhad , H. Toorani (2012). On the postbuckling and free vibrations of FG Timoshenko beams. *Composite Structures,* In Press.

[13] Simsek. M (2010). Non-linear vibration analysis of a functionally graded Timoshenko beam under action of a moving harmonic load. *Composite Structures*, 92, pp. 2532-2546.

[14] Yang.J, Chen Y (2008). Free vibration and buckling analysis of functionally graded beams with edge cracks. *Composite Structures*, 83, pp.48–60.

[15] Yokoyama T (1996). Vibration analysis of Timoshenko beam-columns on two-parameter elastic foundations. *Composite & Structures,* 61, pp. 995-1007.

[16] Wakashima K, Hirano T, Niino M (1990). Space applications of advanced structural materials. ESA, SP, pp. 303 – 97.